

Article

Polyurethane Treated in Ar/C₂H₂/Ar Plasma: Towards Deformable Coating with Improved Albumin Adsorption

Ilya A. Morozov ^{1,2,*} , Alexander S. Kamenetskikh ³, Anton Y. Beliaev ¹, Roman I. Izumov ¹, Marina G. Scherban ⁴, Larisa M. Lemkina ⁵ and Dmitriy M. Kiselkov ⁶

¹ Institute of Continuous Media Mechanics UB RAS, Akademika Koroleva St. 1, 614013 Perm, Russia; belyaev@icmm.ru (A.Y.B.); izumov@icmm.ru (R.I.I.)

² Faculty of Mathematics and Mechanics, Perm State University, Bukireva St. 15, 614990 Perm, Russia

³ Institute of Electrophysics UB RAS, Amundsen St. 106, 620016 Ekaterinburg, Russia; alx@iep.uran.ru

⁴ Faculty of Chemistry, Perm State University, Bukireva St. 15, 614990 Perm, Russia; ma-sher74@mail.ru

⁵ Institute of Ecology and Genetics of Microorganisms UB RAS, Golev St. 15, 614081 Perm, Russia; lemkina46@gmail.com

⁶ Institute of Technical Chemistry UB RAS, Akademika Koroleva St. 3, 614013 Perm, Russia; dkiselkov@yandex.ru

* Correspondence: ilya.morozov@gmail.com

Featured Application: Deformable polymeric devices with improved biomedical properties.

Abstract: Plasma modification of soft polymeric surfaces has many prospects in creating biomedical devices. The deformability of the obtained coatings should be studied, as the usage of such materials implies mechanical loads. Polyurethane (a two-phase synthetic polymer) treated in argon/acetylene plasma, with post-treatment in argon plasma, was investigated. A carbon-containing nanocoating (discontinuous mesh-like structures) with structural–mechanical inhomogeneities is formed by the action of Ar/C₂H₂ plasma. The heterogeneities of the coating are due to the complex structure of the initial substrate and short duration of treatment; as the treatment time increases, the coatings become homogeneous, but their stiffness rises. The treated surfaces in the uniaxial tensile state have micro and/or nanocracks in certain cases of plasma treatment. This is associated with an increased elastic modulus of the coatings. The coatings without cracks have regions with sufficiently alternating stiffness. Post-treatment in argon plasma increases wettability and free surface energy, positively affecting the adsorption of albumin. The stiffness of such coatings increases, becoming more homogeneous, which slightly reduces their crack resistance. Thus, plasma coatings on soft polymers operating under mechanical loads without causing damage should have sufficiently low stiffness, and/or structural-mechanical heterogeneities that provide redistribution of stress.

Keywords: polyurethane; argon; acetylene; plasma; structure; stiffness; proteins; deformation



Citation: Morozov, I.A.; Kamenetskikh, A.S.; Beliaev, A.Y.; Izumov, R.I.; Scherban, M.G.; Lemkina, L.M.; Kiselkov, D.M. Polyurethane Treated in Ar/C₂H₂/Ar Plasma: Towards Deformable Coating with Improved Albumin Adsorption. *Appl. Sci.* **2021**, *11*, 9793. <https://doi.org/10.3390/app11219793>

Academic Editor: Valentina Belova

Received: 1 October 2021

Accepted: 18 October 2021

Published: 20 October 2021

Publisher's Note: MDPI stays neutral with regard to jurisdictional claims in published maps and institutional affiliations.



Copyright: © 2021 by the authors. Licensee MDPI, Basel, Switzerland. This article is an open access article distributed under the terms and conditions of the Creative Commons Attribution (CC BY) license (<https://creativecommons.org/licenses/by/4.0/>).

1. Introduction

To date, a sufficient number of methods of plasma modification of polymers, for improving their biomedical characteristics, have been proposed. One way or another, the treatment affects wettability, free surface energy, chemical structure, and surface topography. As a result, sorption of “good” proteins (e.g., albumin [1,2]) can be improved, which, in turn, affects cell adhesion [3,4]; in certain cases, the amount of “bad” proteins, such as fibrinogen, responsible for thrombosis, is reduced [5,6]. Antibacterial properties may be enhanced due to changes in relief structure [7], wettability [8], and surface chemistry [9]. However, the stiffness of the modified surface often increases. Under certain treatment conditions, when the elastic modulus of the modified layer exceeds that of the polymer material, the surface loses its stability, forming a wrinkled topography. The chaotic structure of the wrinkles has a positive antibacterial effect [10]. This phenomenon has also been found

in applications in metrology [11], the development of smart materials [12], and flexible electronics [13]. However, the application of such materials is associated with mechanical loads that provoke the following defects in the treated surfaces: strain-induced cracks and folds [14–17]. Under cyclic loads, even tiny nanocracks propagate to a considerable depth [18], damaging both the polymer and the surrounding tissues; the formed defects become centers of bacterial growth [10].

Low-energy treatment of the polymer in gaseous plasma, such as argon [19], nitrogen [20], or oxygen [21], is one of the solutions to the problem of the destruction of the modified surface. Note that treatment in plasma of inert gas affects not only the physicochemical properties of the surface, but may reduce the internal stresses in the modified layer [22]. Another way of improving the deformability of coatings is by creating discontinuous (island-like) coatings by plasma chemical deposition of certain species. In particular, the deposition of carbon [23] is of interest. The carbon structure of the coating depends on the choice of carbon-containing reaction gas, treatment, and substrate; diamond-like carbon films [24], fluorocarbons [25], nanotubes, nanofibers, and nanodiamonds [26] may be achieved. The initial stage of coating growth is the nucleation of cores (grains, islets [26]) of the further uniform layer. This stage is of the greatest interest, as it potentially allows deformable heterogeneous coatings with promising properties to be obtained.

Polyurethanes are widespread polymers in many applications; their physical and mechanical properties are determined by the peculiarities of manufacturing. This is a two-phase system consisting of hard blocks in a softer matrix. The aim of this work was to study the changes in the surface properties of polyurethane under the action of argon/acetylene plasma; as a result, carbon-containing nanostructures are formed on the surface. The sorption activity of albumin, as well as the surfaces of the materials in the tensile state, was investigated. The effect of argon post-treatment on modified surfaces is discussed (it is known that argon increases surface activity and may relieve internal stresses in the modified layer).

2. Materials and Methods

Production of polyurethane. Polyurethane was made from a prepolymer (urethane prepolymer based on simple polyester and toluene diisocyanate) and crosslinking agent (hardener MOCA—13.2%, plasticizer polyfurite—84.7%, catalyst voranol—2.1%) in a mass ratio of 100:47. The components were heated to 80 °C and evacuated. The mixture was cured in a mold with an open top at 40 °C for 24 h. The initial elastic modulus measured by uniaxial mechanical test was 8 MPa, elongation at break—900%.

Plasma treatment. The internal two-phase structure of polyurethane is naturally covered by a nanolayer of soft fraction [27]. Low-energy plasma treatment of such surface will only affect this soft layer. Therefore, the surface was pretreated (activated) in plasma of argon for 30 s; studies have shown the etching of the upper layer. Then this surface was treated in argon/acetylene plasma.

The entire treatment cycle is the following: The chamber was evacuated to a pressure of 5×10^{-5} Torr. Argon pressure of 2×10^{-3} Torr was set and a glow discharge was ignited in a low-energy source of an electron beam. The accelerating voltage of electron source was set to 100 V and the discharge—1 A. After treatment in Ar plasma for 30 s, C₂H₂ was pumped into the working chamber at a flow rate of 1 cm³/min. Samples were exposed to Ar/C₂H₂ plasma for 30, 60 or 120 s.

After Ar/C₂H₂ modification, a portion of the samples was post-treated in argon plasma. For this reason, the C₂H₂ flow was stopped and the Ar plasma treatment was continued for 30 s. The purpose of this post-treatment was the possible reactivation of the surface.

Sorption of albumin. An aqueous solution of 1 mg/mL of human albumin (Biolot, Saint Petersburg, Russia) was used. The samples were thermostatted in the solution at 37 °C for 2 h. Concentration of albumin attached to the surface was determined by UV

1080 spectrophotometer (Shimadzu, Kyoto, Japan) at 280 nm as the difference between control (clear solution) and experimental concentrations.

Wetting and free surface energy. The wetting contact angle was determined by a sessile drop method. Water and diethylene glycol were used as test liquids (we did not use diiodmethane, since this and other solvents react with the polymer); the drop sizes were 2–3 mm. The free surface energy was calculated by the Owens–Wendt–Rabel–Caelle method as the sum of the dispersion (accounts van der Waals interactions) and polar (dipole interactions and energy of hydrogen bonds) components. It is known that surface activity of a plasma-treated surface falls to equilibrium for several days, thus the wetting measurements were conducted ten days after the treatment.

Raman spectroscopy. Raman spectra were obtained on a Bruker Senterra dispersive spectrometer with the following parameters: wavelength of the excitation laser—532 nm; duration of accumulation—1 s; number of accumulations—1600; aperture— $25 \times 1000 \mu\text{m}$. The power of radiation was limited to 0.2 mW preventing destruction of the soft polymer. The baseline was aligned using the adaptive method in the SpectraGryph software.

Atomic force microscopy. The surfaces were examined by an atomic force microscope (AFM) Ntegra Prima (NT-MDT BV, Apeldoorn, the Netherlands) in dynamic and static indentation modes. Probes with calibrated tip geometry and stiffness k of the cantilever were used. Undeformed surfaces as well as materials in static tensile state were investigated.

In the dynamic indentation regime the probe ($k = 0.5 \text{ nN/nm}$, tip radius $R = 4 \text{ nm}$) with high frequency ($\sim 0.5 \text{ kHz}$) presses the surface with a small force of $\sim 5 \text{ nN}$, which does not damage the coating. As a result, each point of the surface has its own force interaction curve; their study gives the physical and mechanical properties of the surface. In this paper, we investigated elastic modulus calculated using the Johnson–Kendall–Roberts model.

Static indentation regime allowed the thickness of the coatings to be evaluated. Stiff probes ($k = 4 \text{ nN/nm}$, $R = 10 \text{ nm}$), slow indentation ($\sim 50 \text{ Hz}$) and significant load ($\sim 150 \text{ nN}$) were applied to make 100 indentations in a square region. The indentation with such a force leaves an imprint on a plasma-treated surface, but the surface of the untreated polymer is restored elastically. Thus, the depth of the imprint gives the thickness of the coating [28].

3. Results and Discussion

The surface of polyurethane is naturally covered by a relatively smooth, soft (elastic modulus—4 MPa) layer that is 4–6 nm thick, hiding the internal heterogeneous structure of the polymer (Figure 1a); stiff fibrils (elastic modulus—11 MPa) are embedded in a softer matrix.

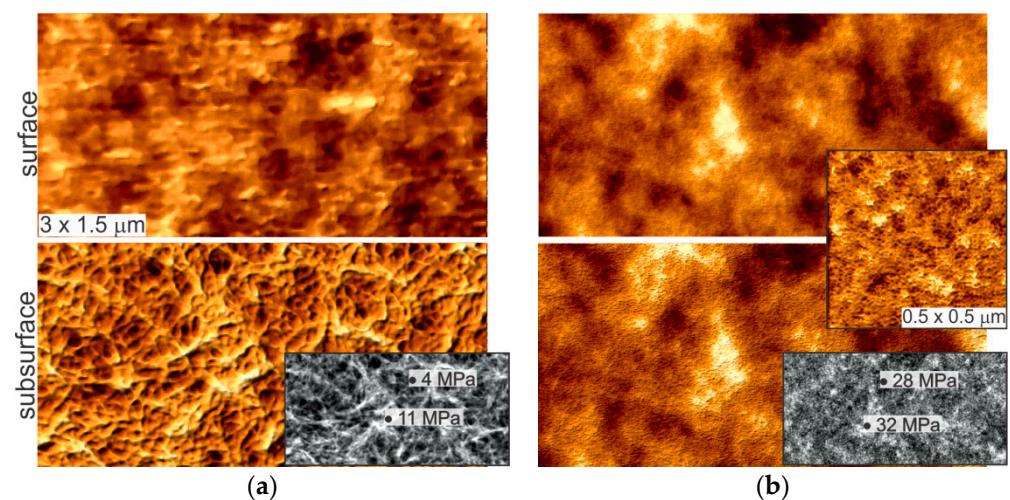


Figure 1. Surface and subsurface of untreated (a) and 30 s treated in argon plasma (b) polyurethane. The insets show maps of the elastic modulus of the subsurface structure. The lighter areas correspond to the stiff objects. The elastic moduli of the typical soft and stiff areas of the surface are marked.

Treatment in argon for 30 s modifies the surface, removing the upper soft layer. The transition between the surface and the subsurface disappears (Figure 1b) and a mesh-like surface nanostructure is formed (see inset in Figure 1b). The stiffness of the surface increases three-fold, becoming more homogeneous; the elastic moduli of the soft and hard areas (see markers in Figure 1) are close. The contrast of structural–mechanical properties is relevant to the untreated polymer; stiffer elevations (agglomerates of the hard fibrils) surrounded by softer depressions (soft areas between hard blocks of the polyurethane) are visible.

The surface changed insignificantly after a short treatment in Ar/C₂H₂ plasma (Figure 2a); the cellular nanostructure is preserved, but the surface stiffness becomes higher and more heterogeneous. Longer treatment times lead to the formation of a coating with structural and mechanical inhomogeneities (Figure 2b,c), where mesh-like areas alternate with smooth areas. The mechanical uniformity of the coating grows; the stiffness of the soft areas increases and approaches the elastic modulus of the stiff areas. The mismatch between surface and substrate stiffness is the reason for the folded topography (see insets in Figure 2), due to the loss of stability of the hard layer on the softer substrate. Argon post-treatment (Figure 2d–f) affects the surface roughness, partially destructs the mesh-like structures, and slightly increases the elastic modulus of the surface.

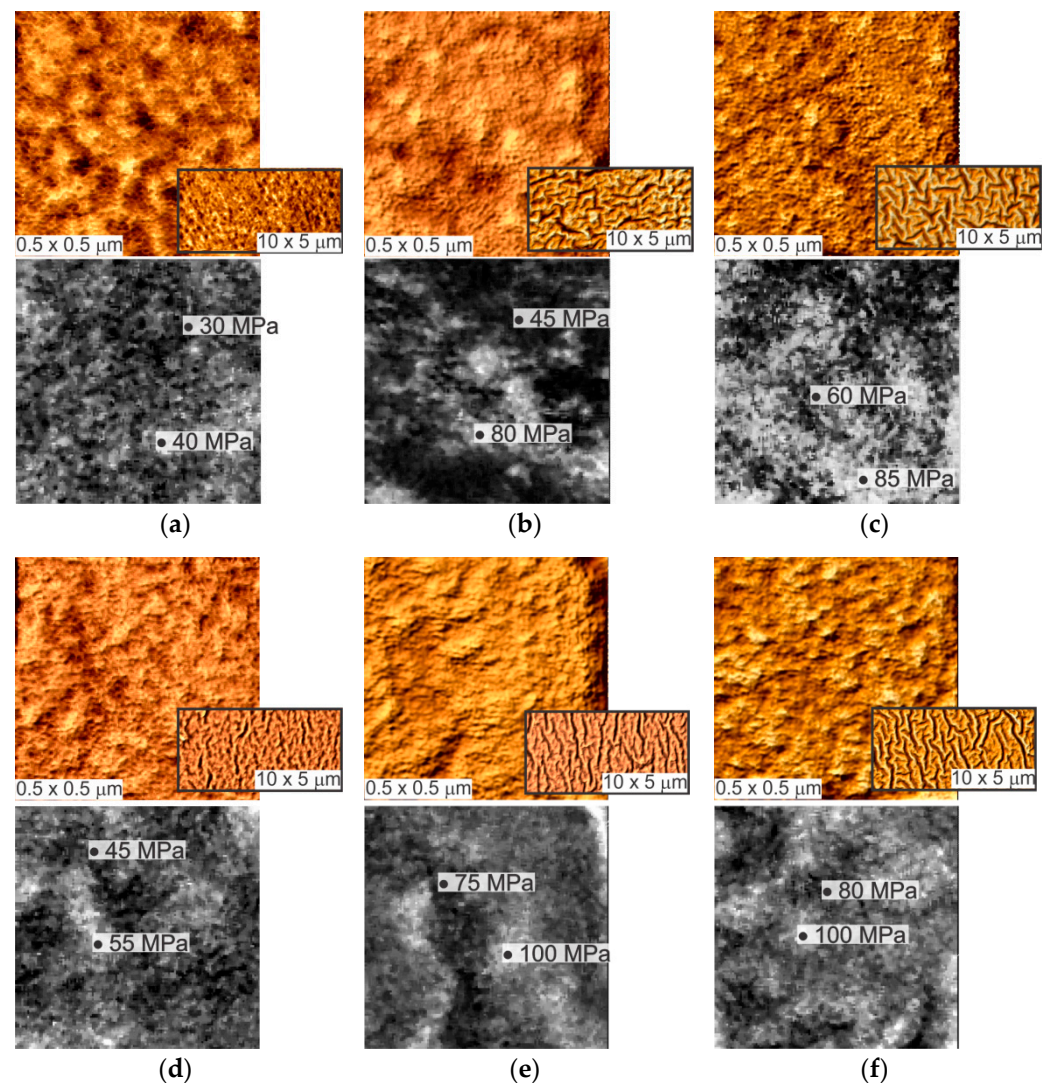


Figure 2. Surface topography and elastic modulus maps of polyurethane treated in Ar/C₂H₂ plasma for 30 s (a), 60 s (b), 120 s (c) and after argon post-treatment (d–f).

The average thickness of the obtained coatings (Figure 3a) grows fast during 30–60 s of treatment in Ar/C₂H₂ plasma; this process slows down in the interval of 60–120 s, which is explained by the densification and homogenization of the coating. Subsequent argon treatment leads to leveling of the coating thickness to ~3.5 nm. Significant scattering of the thickness values is associated with the heterogeneity of the coating at the initial stage of formation, which, in turn, is due to the complex structure of the polyurethane.

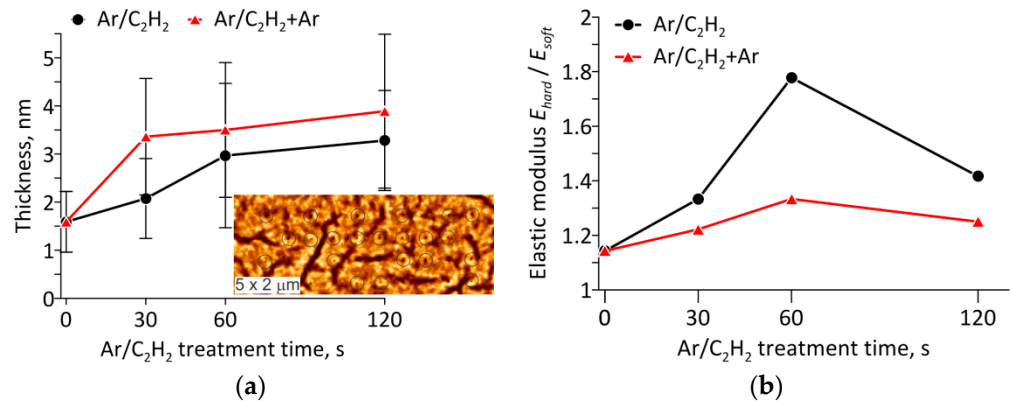


Figure 3. Thickness (a) and ratio of elastic modulus of hard/soft areas (b) of the obtained coatings. Zero treatment time corresponds to the argon plasma-activated polyurethane surface. The inset in (a) shows a fragment of relief with circled indentation imprints whose depth was used for the thickness estimation.

The contrast of the elastic modulus of Ar/C₂H₂-modified surfaces is related both to inhomogeneities of the polymeric substrate and to the non-uniformity of the coating at the initial stage of its formation. The highest scattering of local stiffness is achieved after 60 s of Ar/C₂H₂ treatment (Figure 3b). The argon post-treatment smooths the mechanical properties of the surface; the ratio of hard/soft modulus becomes less pronounced. Note that the modulus of the initially softer areas grows fast, and the modulus of the initially stiff areas increases insignificantly.

In comparison with pristine polymer, plasma treatment increases wettability (Figure 4a) and free surface energy (Figure 4b). The values for Ar/C₂H₂ are slightly worse than after initial argon activation, but the post-treatment by argon leads to a significant decrease in the water contact angle (and rise in free surface energy) for the materials with 30–60 s of Ar/C₂H₂ treatment. The increase in free surface energy is due to the dispersion component of the energy (Figure 4b), which is determined by the action of van der Waals interactions. The polar part of the energy (dipole interactions and the energy of hydrogen bonds) decreases as Ar/C₂H₂ treatment time grows. However, argon post-treatment boosts the polar component at the interval of 30–60 s of Ar/C₂H₂ treatment.

Raman spectroscopy (Figure 4c) reveals changes in the intensity of benzene ring modes (1200, 1258, 1625, 2876, 2936 cm⁻¹), N-C-N (1318 cm⁻¹) [29], and CH₂ (2876 and 2936 cm⁻¹) structures of the polyurethane. Peaks in the 1400–1600 and 2800 cm⁻¹ regions indicate the presence of amorphous carbon film [30,31]. Post-treatment by argon partially destructs the formed chemical structures (the intensity of the corresponding peaks is decreased). A more detailed analysis of the chemical structure of the surface is hampered by the complex structure of the pristine polyurethane and the heterogeneity of the nanocoating.

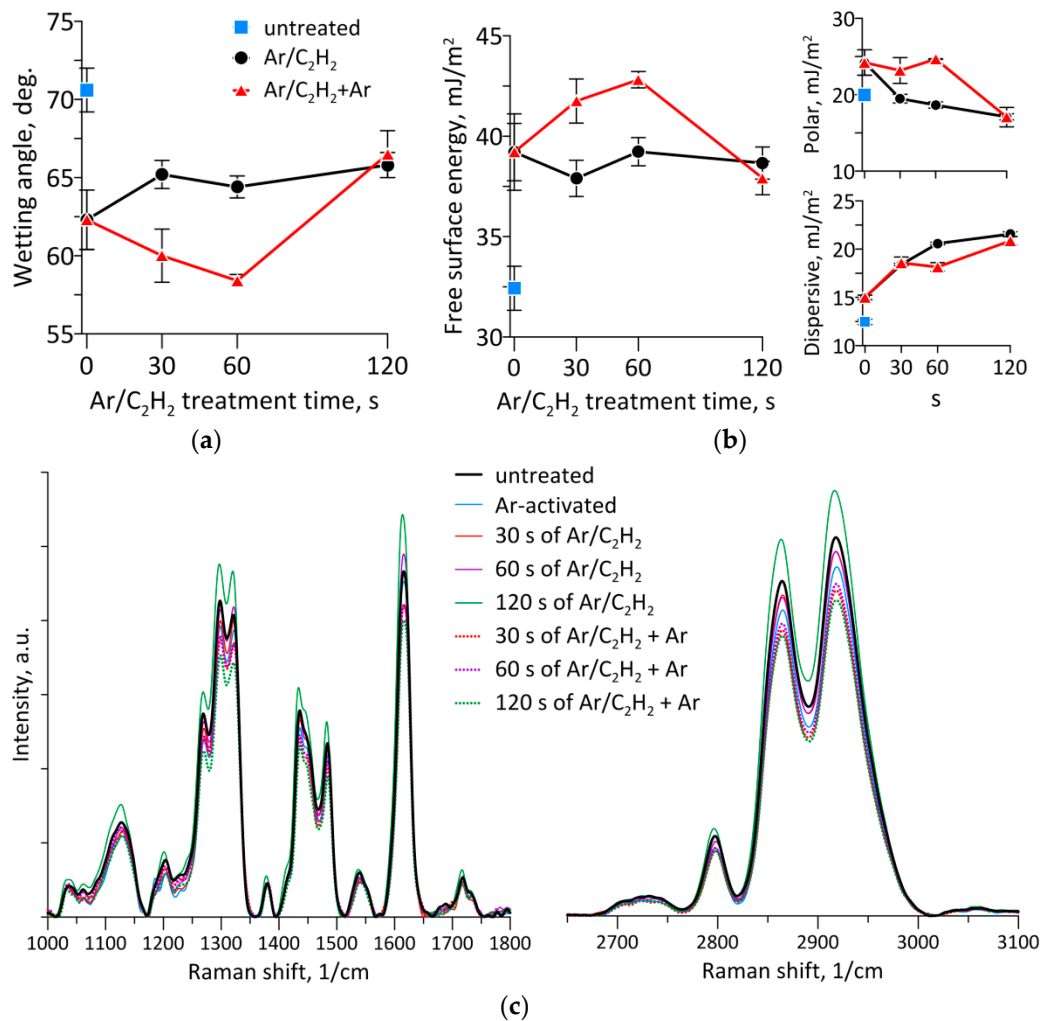


Figure 4. Wetting contact angle (a), free surface energy (b) and Raman spectroscopy (c).

The sorption of proteins onto the surface nonlinearly depends on the combination of wettability [32], free surface energy (in particular, albumin is sensitive to the polar energy component [33]), and roughness [34] (the roughness affects the available area, but may also change the conformation of protein molecules). In our case, albumin sorption was positively affected by the argon post-treatment of Ar/C₂H₂ coatings (Figure 5). The reasons for this are the wettability as well as the polar component of the free surface energy.

Local physical and chemical heterogeneities of pristine polyurethane, as well as after Ar/C₂H₂, hamper the uniform adhesion of albumin on the surface—the nanostructures of protein films have heterogeneities, but argon post-treatment makes the protein layer smooth and uniform (see images in Figure 5).

Micro- and nanocracks are visible on uniaxially deformed (50% of elongation) surfaces after certain cases of treatment (Figure 6). The study of untreated stretched polyurethane, as well as after argon activation, did not reveal any surface defects (these images are not presented).

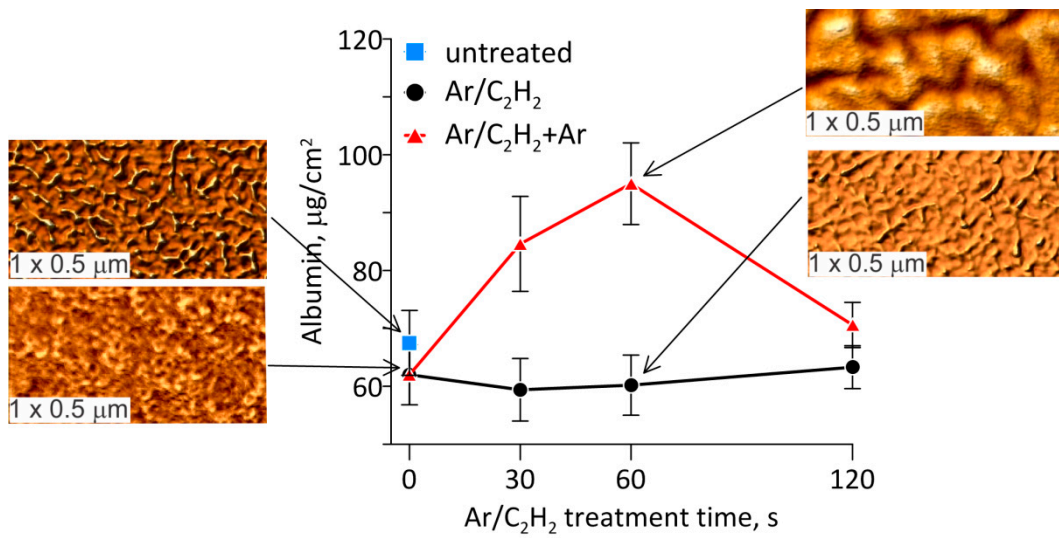


Figure 5. Sorption activity of albumin to the surfaces. The insets show AFM images of surfaces with albumin.

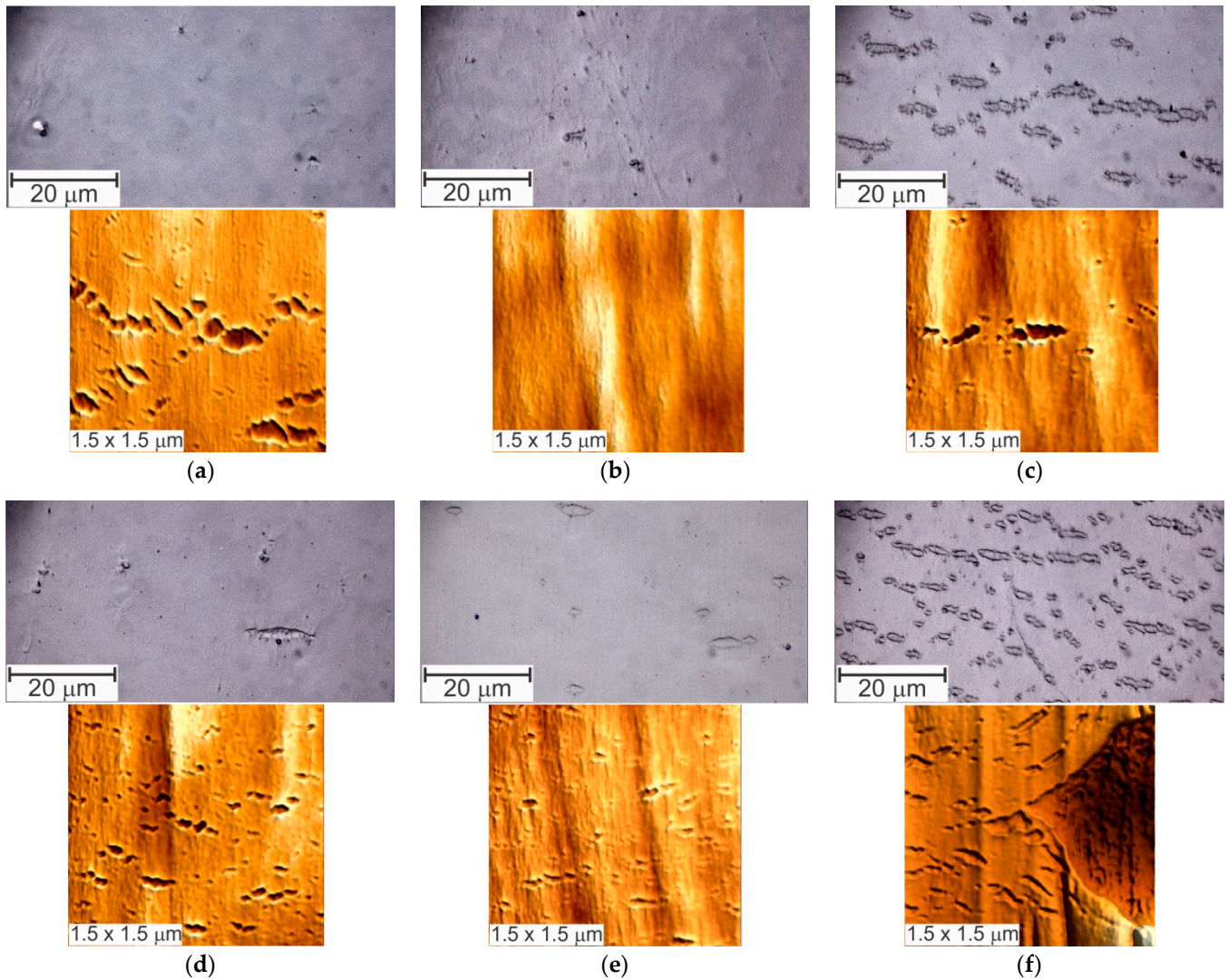


Figure 6. Representative optical images ($70 \times 45 \mu\text{m}$) and AFM images of surfaces stretched to 50%: treatment in Ar/C₂H₂ plasma for 30 s (a), 60 s (b), 120 s (c) and after subsequent argon treatment (d–f). The tensile axis is vertical.

Only one material (60 s of Ar/C₂H₂ treatment, Figure 6b) has no strain-induced cracks at all. This can be explained by the presence of pronounced stiff and soft areas on this surface (Figure 3b); such stiffness mismatches similarly to filler in a polymeric composite and redistributes a load. The rest of the cases show nanocracks (Figure 6a) accompanied by individual microcracks (Figure 6d,e) or a network of microcracks (Figure 6c–f). The increase in the density of cracks is associated with a rise in the elastic modulus of the coatings, as well as with local mechanical inhomogeneities (Figures 2 and 3b).

Crack resistance falls slightly after argon post-treatment (the number of cracks and their sizes become higher) due to the elevated stiffness and uniformity of the coatings. The formation of cracks may lead to undesirable consequences during long-term operation of the material under real conditions. This phenomenon requires a separate study.

4. Conclusions

Elastic polyurethane is a synthetic two-phase polymer that is widely used in various applications. The functional properties of the polymer, in particular, the biocompatibility, can be improved by plasma treatment.

As a result of treatment in Ar/C₂H₂ plasma, a carbon-containing coating of 1.5–3 nm thickness is formed on the polymer surface. The structural and mechanical heterogeneities of the coating are due to the complex structure of the initial polyurethane and the short treatment times. The initial stage of treatment, when a discontinuous inhomogeneous coating with low stiffness is formed, is of great interest. In this case, the modified surface is the most resistant to the strain-induced defects (local micro- and nanocracks) caused by mechanical deformation of the material. Such coatings have improved wettability and increased free surface energy. Argon post-treatment enhances these properties, as well as smooths the structural and mechanical heterogeneities of the surface; all this positively affects the sorption of albumin. However, argon post-treatment leads to higher and more uniform stiffness of the coatings; this slightly reduces the crack resistance of the materials.

The results should be taken into account in the further development of deformable polymeric products for biomedical purposes. The treatment regime should be tuned in such a way as to ensure minimal damage and hardening of the coating, while maximizing the required functional parameters.

Author Contributions: Conceptualization, writing—original draft preparation, I.A.M.; methodology, A.S.K.; investigation, A.Y.B., R.I.I., M.G.S., L.M.L. and D.M.K. All authors have read and agreed to the published version of the manuscript.

Funding: This research was funded by Russian Science Foundation, grant number 17-7920042.

Institutional Review Board Statement: Not applicable.

Informed Consent Statement: Not applicable.

Data Availability Statement: The data presented in this study are available on request from the corresponding author.

Conflicts of Interest: The authors declare no conflict of interest.

References

1. Stüber, M.; Niederberger, L.; Danneil, F.; Leiste, H.; Ulrich, S.; Welle, A.; Marin, M.; Fischer, H. Surface topography, surface energy and wettability of magnetron-sputtered amorphous carbon (a-C) films and their relevance for platelet adhesion. *Adv. Eng. Mater.* **2007**, *9*, 1114–1122. [[CrossRef](#)]
2. Ishige, H.; Akaike, S.; Hayakawa, T.; Hiratsuka, M.; Nakamura, Y. Evaluation of protein adsorption to diamond-like carbon (DLC) and fluorinated DLC films using the quartz crystal microbalance method. *Dent. Mater. J.* **2019**, *38*, 424–429. [[CrossRef](#)] [[PubMed](#)]
3. Zelzer, M.; Albutt, D.; Alexander, M.R.; Russell, N.A. The role of albumin and fibronectin in the adhesion of fibroblasts to plasma polymer surfaces. *Plasma Process. Polym.* **2012**, *9*, 149–156. [[CrossRef](#)]
4. Recek, N. Biocompatibility of plasma-treated polymeric implants. *Materials* **2019**, *12*, 240. [[CrossRef](#)] [[PubMed](#)]
5. Yang, P.; Huang, N.; Leng, Y.X.; Yao, Z.Q.; Zhou, H.F.; Maitz, M.; Leng, Y.; Chu, P.K. Wettability and biocompatibility of nitrogen-doped hydrogenated amorphous carbon films: Effect of nitrogen. *Nucl. Instrum. Meth. B* **2006**, *242*, 22–25. [[CrossRef](#)]

6. Alekhin, A.P.; Boleiko, G.M.; Gudkova, S.A.; Markeev, A.M.; Sigarev, A.A.; Toknova, V.F.; Kirilenko, A.G.; Lapshin, R.V.; Kozlov, E.N.; Tetyukhin, D.V. Synthesis of biocompatible surfaces by nanotechnology methods. *Nanotechnologies Russ.* **2010**, *5*, 696–708. [[CrossRef](#)]
7. Morozov, I.A.; Mamaev, A.S.; Osorgina, I.V.; Lemkina, L.M.; Korobov, V.P.; Belyaev, A.Y.; Porozova, S.E.; Sherban, M.G. Structural-mechanical and antibacterial properties of a soft elastic polyurethane surface after plasma immersion N2+ implantation. *Mat. Sci. Eng. C-Mater.* **2016**, *62*, 242–248. [[CrossRef](#)] [[PubMed](#)]
8. Katsikogianni, M.G.; Missirlis, Y.F. Interactions of bacteria with specific biomaterial surface chemistries under flow conditions. *Acta Biomater.* **2010**, *6*, 1107–1118. [[CrossRef](#)]
9. Patel, J.D.; Ebert, M.; Ward, R.; Anderson, J.M.S. epidermidis biofilm formation: Effects of biomaterial surface chemistry and serum proteins. *J. Biomed. Mater. Res. A* **2007**, *80*, 742–751. [[CrossRef](#)]
10. Morozov, I.A.; Kamenetskikh, A.S.; Beliaev, A.Y.; Scherban, M.G.; Lemkina, L.M.; Eroshenko, D.V.; Korobov, V.P. The effect of damage of a plasma-treated polyurethane surface on bacterial adhesion. *Biophysics* **2019**, *64*, 527–535. [[CrossRef](#)]
11. Chung, J.Y.; Nolte, A.J.; Stafford, C.M. Surface wrinkling: A versatile platform for measuring thin-film properties. *Adv. Mater.* **2011**, *23*, 349–368. [[CrossRef](#)]
12. Zhang, H.; Zhu, H.; Liang, X.; Liu, P.; Zhang, Q.; Zhu, S. Wrinkled smart surfaces: Enhanced switchable wettability and directional liquid transportation. *Appl. Surf. Sci.* **2020**, *513*, 145810. [[CrossRef](#)]
13. Khang, D.Y.; Rogers, J.A.; Lee, H.H. Mechanical buckling: Mechanics, metrology, and stretchable electronics. *Adv. Funct. Mater.* **2009**, *19*, 1526–1536. [[CrossRef](#)]
14. Volynskii, A.L.; Panchuk, D.A.; Sadakbaeva, Z.K.; Bol'shakova, A.V.; Keчек'yan, A.S.; Yarysheva, L.M.; Bakeev, N.F. Formation of a regular microrelief in deformation of plasma-treated polymer films. *Dokl. Phys. Chem.* **2009**, *427*, 133–135. [[CrossRef](#)]
15. Panchuk, D.A.; Sadakbaeva, Z.K.; Bagrov, D.V.; Keчек'yan, A.S.; Bol'shakova, A.V.; Abramchuk, S.S.; Yarysheva, L.M.; Volynskii, A.L.; Bakeev, N.F. Specific features of surface structuring during deformation of plasma-treated polymer films. *Polym. Sci. Ser. A+* **2010**, *52*, 794–800. [[CrossRef](#)]
16. Tsubone, D.; Hasebe, T.; Kamijo, A.; Hotta, A. Fracture mechanics of diamond-like carbon (DLC) films coated on flexible polymer substrates. *Surf. Coat. Tech.* **2007**, *201*, 6423–6430. [[CrossRef](#)]
17. Chudinov, V.; Kondyurina, I.; Terpugov, V.; Kondyurin, A. Weakened foreign body response to medical polyurethane treated by plasma immersion ion implantation. *Nucl. Instrum. Meth. B* **2019**, *440*, 163–174. [[CrossRef](#)]
18. Morozov, I.A.; Mamaev, A.S.; Bannikov, M.V.; Beliaev, A.Y.; Osorgina, I.V. The fracture of plasma-treated polyurethane surface under fatigue loading. *Coatings* **2018**, *8*, 75. [[CrossRef](#)]
19. Alves, P.; Pinto, S.; de Sousa, H.C.; Gil, M.H. Surface modification of a thermoplastic polyurethane by low-pressure plasma treatment to improve hydrophilicity. *J. Appl. Polym. Sci.* **2011**, *122*, 2302–2308. [[CrossRef](#)]
20. Sanchis, M.R.; Calvo, O.; Fenollar, O.; Garcia, D.; Balart, R. Characterization of the surface changes and the aging effects of low-pressure nitrogen plasma treatment in a polyurethane film. *Polym. Test.* **2008**, *27*, 75–83. [[CrossRef](#)]
21. Ozdemir, Y.; Hasirci, N.; Serbetci, K. Oxygen plasma modification of polyurethane membranes. *J. Mater. Sci.-Mater. Med.* **2002**, *13*, 1147–1152. [[CrossRef](#)]
22. Bilek, M.M.M.; McKenzie, D.R. A comprehensive model of stress generation and relief processes in thin films deposited with energetic ions. *Surf. Coat. Technol.* **2006**, *200*, 4345–4354. [[CrossRef](#)]
23. Michelmore, A.; Whittle, J.D.; Short, R.D. The importance of ions in low pressure PECVD plasmas. *Front. Phys.* **2015**, *3*, 1–5. [[CrossRef](#)]
24. Cuong, N.K.; Tahara, M.; Yamauchi, N.; Sone, T. Diamond-like carbon films deposited on polymers by plasma-enhanced chemical vapor deposition. *Surf. Coat. Technol.* **2003**, *174–175*, 1024–1028. [[CrossRef](#)]
25. Barz, J.; Haupt, M.; Oehr, C.; Hirth, T.; Grimmer, P. Stability and water wetting behavior of superhydrophobic polyurethane films created by hot embossing and plasma etching and coating. *Plasma Process. Polym.* **2019**, *16*, 1800214. [[CrossRef](#)]
26. Carvalho, F.H.O.; Vaz, A.R.; Moshkalev, S.; Gelamo, R.V. Synthesis of carbon nanostructures near room temperature using microwave PECVD. *Mater. Res.* **2015**, *18*, 860–866. [[CrossRef](#)]
27. Morozov, I.A. Nanoindentation of polyurethane with phase-separated fibrillar structure. *Polym. Test.* **2021**, *94*, 107038. [[CrossRef](#)]
28. Morozov, I.A.; Kamenetskikh, A.S. Structural-mechanical AFM study of inhomogeneous stiff nanocoating of soft polymer substrate. *IOP Conf. Ser.-Mat. Sci.* **2019**, *699*, 012031. [[CrossRef](#)]
29. Miller, C.E.; Archibald, D.D.; Myrick, M.L.; Angel, S.M. Determination of physical properties of reaction-injection-molded polyurethanes by NIR-FT-Raman spectroscopy. *Appl. Spectrosc.* **1990**, *44*, 1297–1300. [[CrossRef](#)]
30. Chu, P.K.; Li, L. Characterization of amorphous and nanocrystalline carbon films. *Mater. Chem. Phys.* **2006**, *96*, 253–277. [[CrossRef](#)]
31. Wu, J.-B.; Lin, M.-L.; Cong, X.; Liu, H.-N.; Tan, P.-H. Raman spectroscopy of graphene-based materials and its applications in related devices. *Chem. Soc. Rev.* **2018**, *47*, 1822–1873. [[CrossRef](#)] [[PubMed](#)]
32. Jeyachandran, Y.L.; Mielczarski, E.; Rai, B.; Mielczarski, J.A. Quantitative and qualitative evaluation of adsorption/desorption of bovine serum albumin on hydrophilic and hydrophobic surfaces. *Langmuir* **2009**, *25*, 11614–11620. [[CrossRef](#)]

-
33. Michiardi, A.; Aparicio, C.; Ratner, B.D.; Planell, J.A.; Gil, J. The influence of surface energy on competitive protein adsorption on oxidized NiTi surfaces. *Biomaterials* **2007**, *28*, 586–594. [[CrossRef](#)]
 34. Akkas, T.; Citak, C.; Sirkecioglu, A.; Güner, F.S. Which is more effective for protein adsorption: Surface roughness, surface wettability or swelling? Case study of polyurethane films prepared from castor oil and poly(ethylene glycol): Protein adsorption on polyurethane films. *Polym. Int.* **2013**, *62*, 1202–1209. [[CrossRef](#)]